Testosterone and 17β-Estradiol Induce Glandular Prostatic Growth, Bladder Outlet Obstruction, and Voiding Dysfunction in Male Mice

Tristan M. Nicholson, Emily A. Ricke, Paul C. Marker, Joseph M. Miano, Robert D. Mayer, Barry G. Timms, Frederick S. vom Saal, Ronald W. Wood, and William A. Ricke

Department of Urology and Carbone Cancer Center (T.M.N., E.A.R., W.A.R.), Division of Pharmaceutical Sciences (P.C.M.), University of Wisconsin, Madison, Wisconsin 53705; Departments of Pathology and Laboratory Medicine (T.M.N.), Urology (R.D.M., R.W.W.), Obstetrics and Gynecology (R.W.W.), Neurobiology and Anatomy (R.W.W.), and Medicine (J.M.M.) and Aab Cardiovascular Research Institute (J.M.M.), University of Rochester Medical Center, Rochester, New York 14642; Division of Basic Biomedical Sciences (B.G.T.), University of South Dakota, Vermillion, South Dakota 57069; and Division of Biological Sciences (F.S.v.S.), University of Missouri, Columbia, Missouri 65211

Benign prostatic hyperplasia (BPH) and bladder outlet obstruction (BOO) are common in older men and can contribute to lower urinary tract symptoms that significantly impact quality of life. Few existing models of BOO and BPH use physiological levels of hormones associated with disease progression in humans in a genetically manipulable organism. We present a model of BPH and BOO induced in mice with testosterone (T) and 17β-estradiol (E_2). Male mice were surgically implanted with slow-releasing sc pellets containing 25 mg T and 2.5 mg E_2 (T+E_2). After 2 and 4 months of hormone treatment, we evaluated voiding patterns and examined the gross morphology and histology of the bladder, urethra, and prostate. Mice treated with T+E_2 developed significantly larger bladders than untreated mice, consistent with BOO. Some mice treated with T+E_2 had complications in the form of bladder hypertrophy, diverticula, calculi, and eventual decompensation with hydronephrosis. Hormone treatment caused a significant decrease in the size of the urethral lumen, increased prostate mass, and increased number of prostatic ducts associated with the prostatic urethra, compared with untreated mice. Voiding dysfunction was observed in mice treated with T+E_2, who exhibited droplet voiding pattern with significantly decreased void mass, shorter void duration, and fewer sustained voids. The constellation of lower urinary tract abnormalities, including BOO, enlarged prostates, and voiding dysfunction seen in male mice treated with T+E_2 is consistent with BPH in men. This model is suitable for better understanding molecular mechanisms and for developing novel strategies to address BPH and BOO. (*Endocrinology* 153: 5556–5565, 2012)

Benign prostatic hyperplasia (BPH) is prevalent among older men and increases with age; it is found at autopsy in approximately 70% of men in their sixties and up to 90% of men in their eighties (1). BPH develops in the transition zone of the prostate surrounding the proximal urethra and as the prostate enlarges it may impede urine flow, leading to bladder outlet obstruction (BOO), which can cause or contribute to bothersome lower urinary tract symptoms (LUTS). LUTS encompass a range of clinical complaints, including weak stream, straining to urinate, incomplete bladder emptying, frequency, urgency, nocturia, and small voided volumes (2). In addition to LUTS, urinary tract complications can occur in the setting of BOO due to BPH, including elevated postvoid residual,

Abbreviations: ACTA2, α-Actin; BOO, bladder outlet obstruction; BPH, benign prostatic hyperplasia; DHT, 5α-dihydrotestosterone; E_2, 17β-estradiol; H&E, hematoxylin and eosin; LUTS, lower urinary tract symptoms; MYH11, myosin heavy chain; T, testosterone.

urinary retention, bladder diverticula, hydronephrosis, bladder calculi, and renal insufficiency (3). These conditions significantly affect the quality of life of a substantial proportion of men, and the associated healthcare costs are in the billions annually (4–6). The natural history of male LUTS is variable, but when untreated, obstructive symptoms (weak stream, straining, and incomplete emptying) and nocturia tend to worsen with age as the prostate enlarges (7). An animal model that recapitulates the pathophysiology of BPH, BOO, and voiding dysfunction could provide important clues for understanding the molecular mechanisms underlying the etiology of these common clinical problems. Previous animal models of partial BOO, by causing partial obstruction of the bladder outlet with sutures or cuffs, have advanced understanding of the bladder's response to acute obstruction, such as detrusor hypertrophy and decompensation (8–11). Because BPH in men is a disease process that likely develops over decades, a model of gradual obstruction may be more relevant to improve understanding of BOO associated with BPH.

Sex steroid hormones have long been implicated in the development of BPH and its clinical sequelae (12). Androgens are essential for prostate development and growth and their effects depend on interaction with the androgen receptor (13). Additionally it is known that castrated men do not develop prostatic hyperplasia (14). The testosterone (T) metabolite 5α-dihydrotestosterone (DHT) is the major androgen acting on the prostate, and medical therapy with 5α-reductase inhibitors that block conversion of T to DHT decrease prostate volume, improve symptoms, and increase urinary flow rates in men with LUTS associated with BPH (15, 16). However, complete androgen deprivation does not result in symptomatic improvement in all men, and androgen supplementation of hypogonadal men does not appear to increase the risk of BPH (14, 17). In fact, BPH develops in older men as serum T levels decline (18). With advancing age, serum levels of E_2 can remain relatively constant or increase, but the net effect is a decline in the ratio of free serum T to 17β-estradiol (E_2) that parallels the development of BPH and LUTS (19, 20). The androgen and estrogen balance is well established as important in both prostate development and disease, but the molecular underpinnings of this relationship are not well understood (21). Streng and colleagues (22, 23) have demonstrated that treatment of male Noble rats with pharmacological doses of T and E_2 ($T+E_2$) leads to a decreased serum T to E_2 ratio, induces inflammation in the dorsolateral prostate, and causes obstructive voiding. We have previously described that male mice treated with sc implants of 25 mg T and 2.5 mg E_2 have serum hormone levels similar to physiological hormone levels of aging men (24, 25). Furthermore, male mice treated with $T+E_2$ de-

velop prostatic epithelial hyperplasia, and this effect is observed across several strains of mice (24). However, rodents have generally been thought to be a poor model for BPH/LUTS due to their prostate anatomy, which is dissimilar to that of men. In this paper, we characterize a model of new glandular prostate growth, BOO, and urinary voiding dysfunction in male mice treated with $T+E_2$. By recapitulating the hormonal milieu and many of the clinical features observed in BPH patients, this model may be uniquely suited for future study of the underlying molecular mechanisms of sex steroids in the pathogenesis of BPH.

Materials and Methods

Steroid implantation

C57BL/6 and BALB/c mice (6–8 wk of age) were obtained from Charles River (Wilmington, MA) and reared under standard laboratory conditions (12-h light, 12-h dark cycle) with free access to food and water. Laboratory Animal Resources staff of the University of Rochester and University of Wisconsin School of Medicine and Public Health provided routine care. All animal experiments and procedures were conducted under a protocol approved by the University of Rochester's University Committee on Animal Resources and the University of Wisconsin Animal Care and Use Committee. T and E_2 were obtained from Sigma Chemical Co. (St. Louis, MO). Mice were treated with surgically implanted compressed hormone pellets containing 25 mg T and 2.5 mg E_2 for 2 or 4 months as described previously (25, 26).

Tissue collection

After euthanasia with CO_2 and exsanguination, laparotomy was performed and the bladder was measured *in situ* in three dimensions with a precision caliper. Bladder volume was estimated by calculating the volume of an ellipsoid in cubic millimeters (27). The urogenital tract was dissected, excised, and photographed. The urethra, prostate lobes, and bladder were removed and photographed. The anterior prostate was dissected from the urogenital tract, blotted dry, and weighed. Bladders were drained of urine, blotted dry, and weighed. When present, calculi were removed from the bladder, dried, and photographed before being sent for integrated crystallographic analysis by Louis C. Herring and Co. Analytical and Consulting Chemists (Orlando, FL).

Morphometric analysis

All tissues were fixed in 10% neutral buffered formalin for 24 h at room temperature, dehydrated in ethanol, cleared in xylene, and embedded in paraffin. Transverse sections (6 μm) were cut from the proximal prostatic urethra. For morphometric evaluation, the sections were mounted on slides and every 20th section was stained with hematoxylin and eosin (H&E). Stained sections were viewed with a Leica DM5000 B digital microscope at ×5 magnification and photographed with a Leica CTR 500 digital camera (Leica Microsystems, Wetzlar, Germany). The microscope was calibrated with a 1-mm scale slide. Images were acquired using PictureFrame version 2.3 (Optronics, Goleta,

CA) and analyzed with ImageJ software (National Institutes of Health, Bethesda, MD). The outline of the urethra, rhabdosphincter, periurethral space, urethral lumen, and bladder detrusor was contoured by hand with a computerized stylus using ImageJ software. The detrusor was contoured by hand in the largest H&E-stained transverse section of the bladders and converted to color shell to determine the area. Areas were measured in pixels squared and converted to square micrometers. A single observer blinded to treatment condition using ImageJ counted prostatic glands/buds manually.

Staining/immunohistochemistry

All procedures were performed as we have described previously (24, 25). To identify connective tissue and muscle, we used a Masson's trichrome stain kit and performed staining according to the manufacturer's protocol (Leica Microsystems). For identification of smooth muscle, sections were first blocked with 5% normal goat serum in 0.1 M PBS. Primary antibodies to the smooth muscle isoforms of myosin heavy chain (MYH11) (Biomedical Technologies, Stoughton, MA; 1:300 dilution) and α-actin (ACTA2) (Dako, Carpinteria, CA; 1:500 dilution) were applied to sections of bladder for 1 h at room temperature. After a 5-min wash in 0.1 M PBS, sections were incubated with biotinylated goat antirabbit IgG (1:100) for 1 h and the avidin-biotin complex (Vector Laboratories, Burlingame, CA) for an additional 1 h. Finally, sections were stained using a Vector red alkaline phosphatase substrate kit (Vector) and then observed under an Olympus BX-41 light microscope (Olympus, Melville, NY).

Uroflow

Our method for evaluating uroflow has been previously described (28, 29). After hormone implantation, mice were placed in Tecniplast (Exton, PA) metabolism cage racks equipped with rat floor grids to minimize urine retention. Mice were offered 6 ml of a preferred solution of 0.25% saccharin and 3% glucose in a double-ball-bearing sipper tube attached to a length of Tygon tubing as a fluid reservoir (30). This was placed in the metabolism cage fluid access recess; the food port was blocked with a plate for the duration of evaluation. Milligram-resolution electronic balances (Mettler, Columbus, OH) and waste plates were placed directly under the floor grids without fecal separation screens. The balances were configured to report current stability status and mass 10 times per second. This character stream was received from an internet port address by a custom program (LabVIEW, National Instruments, Austin, TX) that immediately generated online displays of the record and histograms of void mass, duration, and uroflow. Network cameras (Axis 206, Lund, Sweden) sent synchronous images from below, which were retained as movie files associated with each period of balance instability. This capability allows comparison of the recorded waveforms with synchronized videos of the event. Twenty-four balances were monitored simultaneously from a single remote workstation. Previously published methods from this laboratory used laboratory-dependent waveform smoothing for noise elimination (28, 29). To achieve laboratory independence and to ensure that small voiding events typical of end-stage obstructive dysfunction were not excluded in this process, no waveform smoothing was performed before event detection. Imposing upper and lower limits on the derived measures eliminates vibration

and air current artifacts, and we compared the effect of these with the raw instability event record and associated video records.

Statistics

Data analysis for comparisons of continuous variables consisted of two-tailed unpaired *t* test or one-way ANOVA with Bonferroni *post hoc* comparisons. Bar graphs show means ± SEM. In all analyses, $P < 0.05$ was considered statistically significant.

Results

T+E$_2$ treatment causes enlarged bladders, changes in bladder smooth muscle and collagen, and upper urinary tract complications consistent with BOO

After 2 months of treatment with T+E$_2$, we observed enlarged bladders (Fig. 1A). Treatment with T+E$_2$ for 2 months caused increased bladder mass (+70%), bladder volume (+910%), and cross-sectional area of the detrusor relative to untreated controls (+124%, Table 1, $P < 0.05$). Thickening of the detrusor after 2 months of hormone treatment was observed with H&E-stained sections (Fig. 1A). To evaluate whether our model was accompanied by muscle hypertrophy followed by fibrosis, which can be seen clinically (31), we stained with two markers of smooth muscle (ACTA2 and MYH11) as well as Masson's trichrome, which stains for extracellular matrix including collagen (Fig. 2, C and D). Bladders from untreated mice had little stain for collagen, but the bladders of mice treated for 2 months with T+E$_2$ contained abundant amounts of collagen (*blue* in Fig. 1C). Among the untreated mice and mice treated for 2 months with T+E$_2$, smooth muscle cell markers MYH11 and ACTA2 stained intensely throughout the detrusor (Fig. 1D). After 4 months of treatment with T+E$_2$, we observed very large, distended bladders with residual urine at the time of euthanasia, with thin walls (Fig. 1A). Four months of treatment with T+E$_2$ caused increased bladder mass (+126%) and bladder volume (+6800%) compared with mice untreated for 4 months (Table 1, $P < 0.05$). The cross-sectional area of the detrusor was decreased compared with mice treated with 2 months of hormones (−31%, $P < 0.05$) but was increased relative to untreated controls (+52%, Table 1, $P < 0.05$). After 4 months of hormone treatment, some T+E$_2$-treated mice developed bladder diverticula and hydronephrosis, hallmarks of BOO (Fig. 1B). The bladder of one mouse treated with T+E$_2$ contained multiple irregular calculi, composed of 95% magnesium ammonium phosphate hexahydrate (struvite), 1% carbonate apatite, and 4% protein and blood, which can develop in the setting of urinary status from BOO (Fig. 1B). In bladders from mice treated for 4 months with
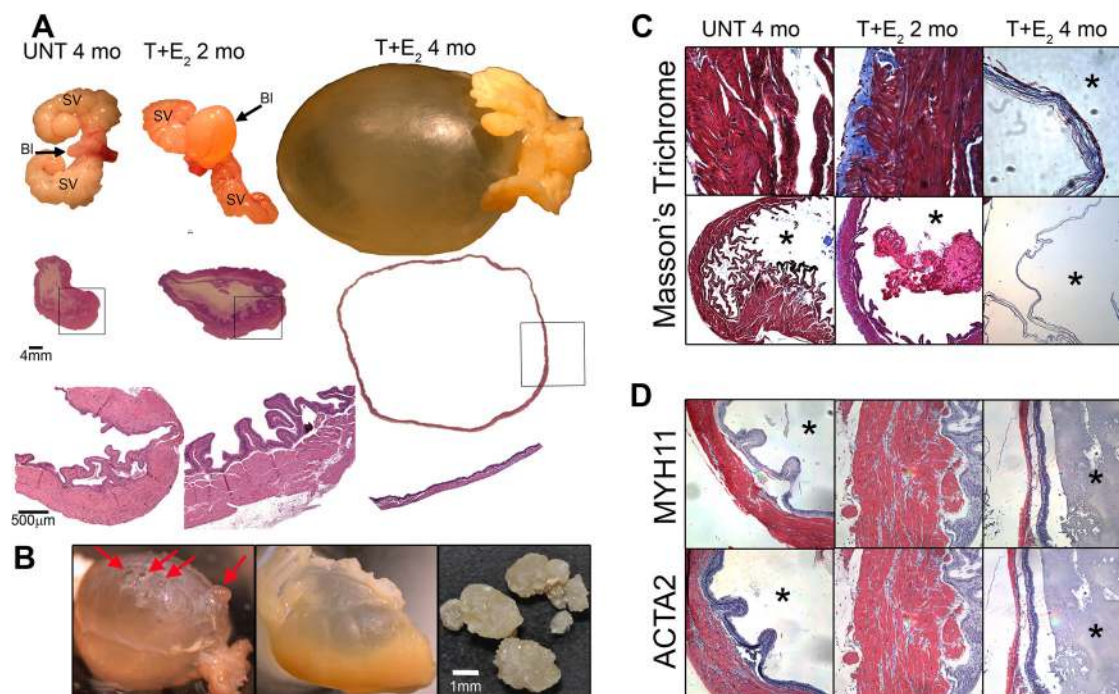
FIG. 1. Effects of T+E_2 treatment on the urinary tract of male C57BL/6 mice. A, After 2 months of treatment with T+E_2, the bladder was somewhat enlarged and contained residual urine compared with the small, deflated bladder of the untreated (UNT) mouse at the time of euthanasia. High-magnification H&E-stained sections (*bottom panels*) of representative mice revealed increased detrusor thickness after 2 months of T+E_2 treatment. Four months of treatment with T+E_2 caused very large bladders distended with large amounts of residual urine. After 4 months of T+E_2 treatment, the bladder was distended with marked thinning of the detrusor seen with H&E staining. Bl, Bladder; SV, seminal vesicles. B, After 4 months of T+E_2 treatment, some mice had bladder diverticula (*red arrows*) and hydronephrosis (*middle panel*), indicating increased intravesical pressure relative to pressure of the ureters and renal pelves. Irregular bladder calculi were occasionally found (*right panel*), indicating urinary stasis in the setting of obstruction. C, Male mice were untreated or treated with T+E_2 for 2 and 4 months, and bladders were processed and stained with Masson's trichrome stain (cells stain red and collagen stains blue). After 2 months of treatment, bladders from T+E_2-treated mice showed increased collagen staining (*blue*), whereas very little collagen was observed in untreated normal bladders. After 4 months of hormone treatment, layers of disorganized collagen had mostly replaced the thinned detrusor. D, Localization of smooth muscle ACTA2 and MYH11 in serial sectioned bladders collected from untreated and T+E_2-treated male mice at 2 and 4 months. After T+E_2 treatment for 2 months, both smooth muscle markers (*red*) stained intensely and were found throughout the thickened detrusor relative to untreated bladders, indicating detrusor hypertrophy. After 4 months of T+E_2-treatment, when distended bladders were observed, very little smooth muscle marker staining was present. This is consistent with the trichrome staining in C where cells (*red*) are primarily found in the urothelium and the stroma is rich with collagen (*blue*) but contains few red stained cells. *, Bladder lumen.

T+E_2, the thinned detrusor was mostly replaced by disorganized collagen (Fig. 1C), and there was very little staining of MYH11 and ACTA2, indicating a change in the compliance of the bladder (Fig. 1D). Other observations among the mice treated with T+E_2 included grossly enlarged seminal vesicles, prostates, and preputial glands and urine-soaked fur near the urethral orifice.

T+E_2 treatment causes urethral narrowing, increased prostate mass and glandular prostatic duct growth

As we have previously described (12), the prostatic urethra was defined as sections of the urethra cranial to the verumontanum containing the ejaculatory ducts and main ducts of the seminal vesicles (Supplemental Fig. 1, pub-

TABLE 1. Effects of T+E_2 treatment on the mouse bladder

	Bladder mass (mg)	Bladder volume (mm³)	Detrusor cross-sectional area (μm²)
UNT 2 months (n = 5)	37.9 ± 2.9	17.9 ± 1.7	
T+E_2 2 months (n = 5)	64.3 ± 6.8[a]	180.8 ± 48.6[a]	9.4 ± 1.0[a]
UNT 4 months (n = 10)	40.6 ± 3.8	23.1 ± 2.9	4.2 ± 0.2
T+E_2 4 months (n = 9)	91.9 ± 7.2[a,b]	1596 ± 352[a,b]	6.4 ± 1.0[a,b]

Values are means ± SEM. UNT, Untreated controls.

[a] $P < 0.05$ compared with respective UNT.

[b] $P < 0.05$ compared with T+E_2 2 months.
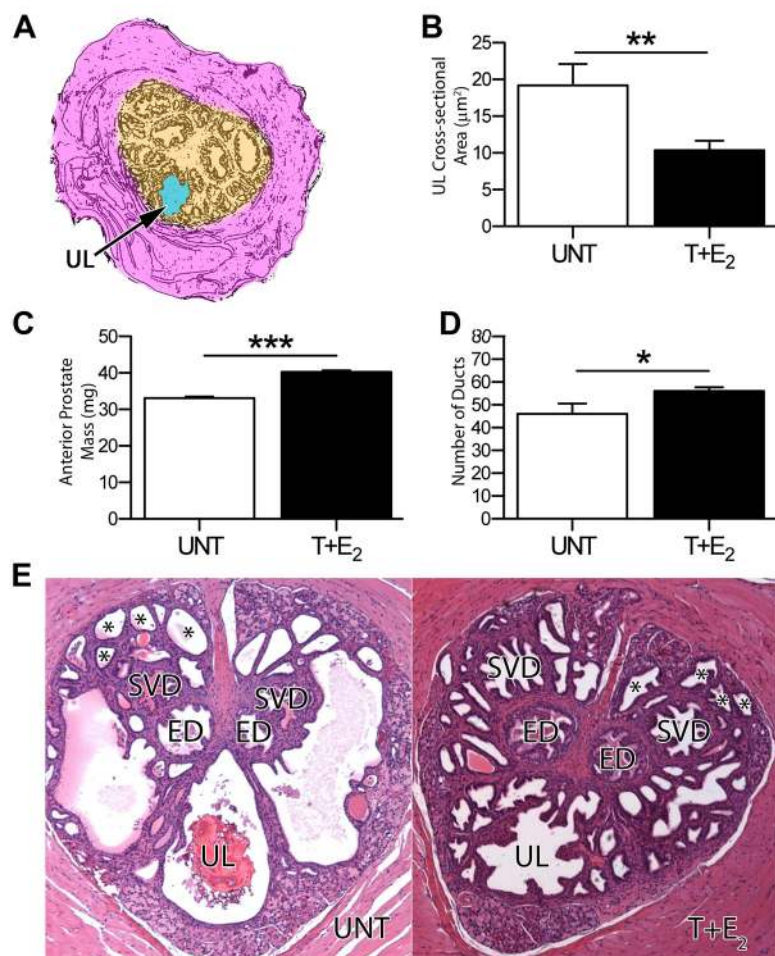
FIG. 2. T+E$_2$ treatment of C57BL/6 mice causes urethral narrowing, increased anterior prostate mass, and increased prostatic ducts in the proximal urethra. A, Measurements were contoured by hand in ImageJ to determine the cross-sectional area of the urethral lumen (*blue*). B, Mice treated with T+E$_2$ for 4 months had a significantly smaller average cross-sectional area of the prostatic urethral lumen compared with untreated controls (**, $P = 0.004$). C, Compared with untreated mice, the mass of the anterior prostate from mice treated with T+E$_2$ for 4 months was significantly greater (***, $P < 0.0001$). D, Mice treated for 4 months with T+E$_2$ had significantly more prostatic ducts in the proximal urethra compared with untreated controls (*, $P = 0.015$). E, Prostatic ducts were counted in a representative section of the prostatic urethra, and untreated mice (*left*) were compared with mice treated with T+E$_2$ for 4 months (*right*). Prostate cancer and prostatic intraepithelial neoplasia were not observed in the urethra.*, Prostatic ducts, ED, ejaculatory ducts; SVD, main seminal vesicle ducts; UL, urethral lumen.

lished on The Endocrine Society's Journals Online web site at http://endo.endojournals.org). Measures of the prostatic urethra consisted of the total cross-sectional area, the rhabdosphincter, periurethral glandular tissue containing prostate ducts (Supplemental Fig.1A), and the urethral lumen (Fig. 2A). There were no significant differences among mice treated with T+E$_2$ compared with untreated controls in the cross-sectional areas of the total prostatic urethra (Supplemental Fig.1B), striated rhabdosphincter (Supplemental Fig.1C), or the periurethral glandular tissue compartment (Supplemental Fig.1D). The average cross-sectional area of the prostatic urethral lumen was

significantly smaller (-46%) among mice treated with T+E$_2$ compared with the untreated controls (Fig. 2B, $P = 0.004$), consistent with BOO. The average mass of the anterior prostate of mice treated with hormones was significantly greater ($+21\%$) than that of untreated controls ($P < 0.001$, Fig. 2C). Treatment with T+E$_2$ also significantly increased the number of prostatic ducts in the prostatic urethra compared with the untreated controls ($+22\%$, $P < 0.05$, Fig. 2 D and E). Prostate cancer and prostatic intraepithelial neoplasia were not observed in the urethra.

T+E$_2$ treatment causes urinary voiding dysfunction in the form of droplet voiding pattern

A typical untreated mouse exhibited several sustained voids per session, whereas a typical mouse treated with T+E$_2$ exhibited small-mass, short-duration voids that consisted of droplets of urine (Fig. 3A). The voiding behavior of the T+E$_2$ mouse in Fig. 3A was classified as droplet voiding pattern, because only droplets of urine were observed as voiding events on synchronized video. Median uroflow curves for individual mice in the study were generated to characterize uroflow patterns based on the shape of these curves. Untreated mice exhibited sustained voiding pattern (Fig. 3B and Supplemental Video 1), whereas mice treated with T+E$_2$ were classified into sustained voiding pattern or droplet voiding pattern based on distinctive median uroflow curves (Fig. 3, B and C). Four of nine mice treated with T+E$_2$ exhibited sustained voiding pattern (Fig. 3C). The remaining five of nine mice treated with T+E$_2$ exhibited median uroflow curves consistent with droplet voiding pattern and predominantly droplet voiding pattern on video (Fig. 3C and Supplemental Video 1). To characterize the distribution of individual urinary voiding events and reveal patterns for individual mice, the duration and mass of all voids recorded were plotted for each mouse (Fig. 4). Among the untreated mice, there was some variability among individual mice in void masses and durations (Fig. 4A). Examination of individual plots of duration and mass for each void showed that four of the mice treated with T+E$_2$ displayed a mixture of sustained voiding pattern and droplet voiding pattern (Fig. 4B). The five mice treated with T+E$_2$ and classified as droplet voiding pattern with median uroflow curves displayed exclusively droplet voiding pattern based on the pattern of void volumes and
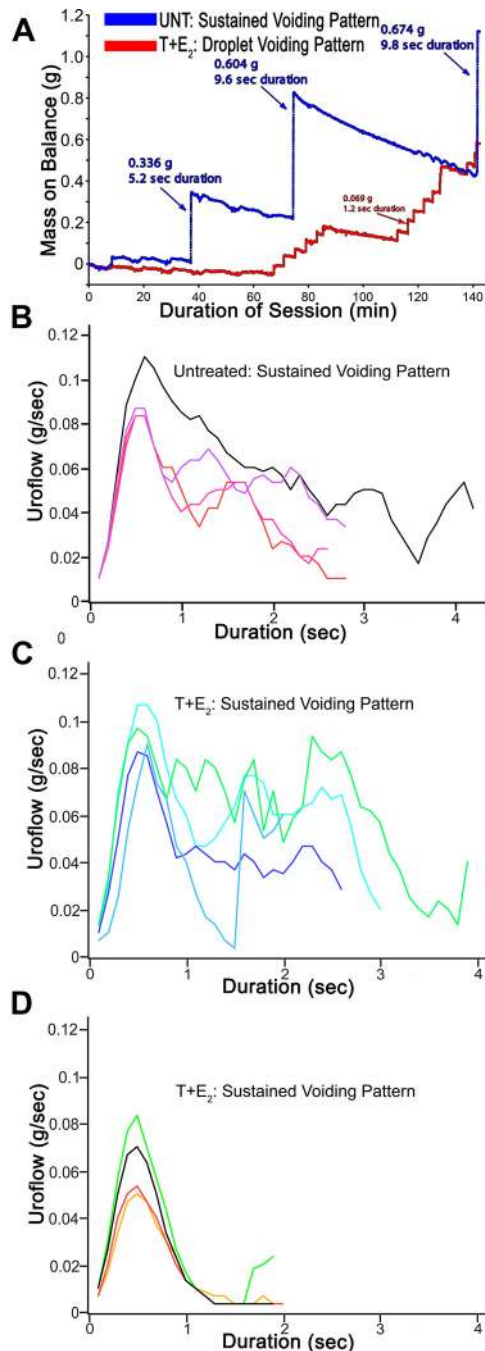
FIG. 3. Treatment of male BALB/c mice with T+E$_2$ causes voiding dysfunction in the form of droplet voiding pattern. A, Representative uroflow session with net mass on balance recorded over time from an untreated mouse (UNT; *blue*) compared with a mouse treated with T+E$_2$ (*red*). The untreated mouse exhibits three sustained voids. The mouse treated with T+E$_2$ has frequent small-mass, short-duration voids. Analysis of a synchronized video stream determined the voiding events in the mouse treated with T+E$_2$ consist of a droplet of urine striking the balance (droplet voiding pattern). B–D, Median uroflow curves reflecting all voids across all sessions from 2–4 months of hormone treatment for all mice in the study (*individual lines* represent individual mice). B, Four untreated mice show median uroflow curves consistent with sustained voiding pattern. C, Four mice treated with T+E$_2$ have median uroflow curves, reflecting sustained voiding pattern, similar to untreated mice in B. D, Among five mice treated with T+E$_2$, median uroflow curves reflect droplet voiding pattern.

durations observed (Fig. 4C). As shown in Table 2, among mice treated with T+E$_2$ compared with untreated mice, the average voided mass was significantly smaller (-32%, $P = 0.003$) and duration of void significantly shorter (-46%, $P = 0.005$). Overall, mice treated with T+E$_2$ exhibited significantly fewer sustained voids (defined as duration > 3 sec and mass >0.10 g; -76%, $P = 0.001$; Table 2).

Discussion

We present a mouse model of male BOO induced by sex steroid hormones that recapitulates many features of men with BPH and LUTS: voiding dysfunction accompanied by detrusor thickening and fibrosis and, in some cases, eventual decompensation, urinary retention, and hydronephrosis. After 2 months of treatment with T+E$_2$, mice developed thickening of the detrusor due to increased smooth muscle and collagen, consistent with hypertrophy and fibrosis induced by BOO. After 4 months of treatment with T+E$_2$, the majority of mice developed gross enlargement of the bladder with a thinned, fibrotic detrusor, and in some mice this was accompanied by evidence of high-pressure storage or voiding in the form of bladder diverticula and hydronephrosis. The presence of bladder stones in one mouse treated with T+E$_2$ is suggestive of urinary stasis, which is a manifestation of BOO in BPH patients.

Due to differences in prostate anatomy, rodents have previously not been considered a useful model for human male BOO and BPH. Dogs and primates are the only mammals known to spontaneously develop symptomatic BPH, and this has been attributed to encapsulation of the prostate by fascial layers, with urethral obstruction occurring as a consequence of increased prostatic tissue mass. Due to this anatomic difference, even when enlarged, the distal murine prostatic lobes would be unlikely to cause BOO. However, an increase in the prostate tissue encapsulated within the thick rhabdosphincter may narrow the urethral lumen and restrict urinary flow and hence might be analogous to BOO found in men due to BPH. Treatment of male mice with T+E$_2$ caused changes in the morphology of the proximal urethra, with an increased number of prostatic ducts and narrowing of the urethral lumen, suggesting that BOO was caused by hormone treatment and implicating these periurethral changes. The finding from this study with the T+E$_2$-treated male mouse is a unique description, to our knowledge, of urethral narrowing associated with stimulation of prostate glandular growth in a murine model system.

Despite anatomic differences, treatment of the male mouse with T+E$_2$ recapitulates the major clinical manifestation of BPH in men: urinary voiding dysfunction.
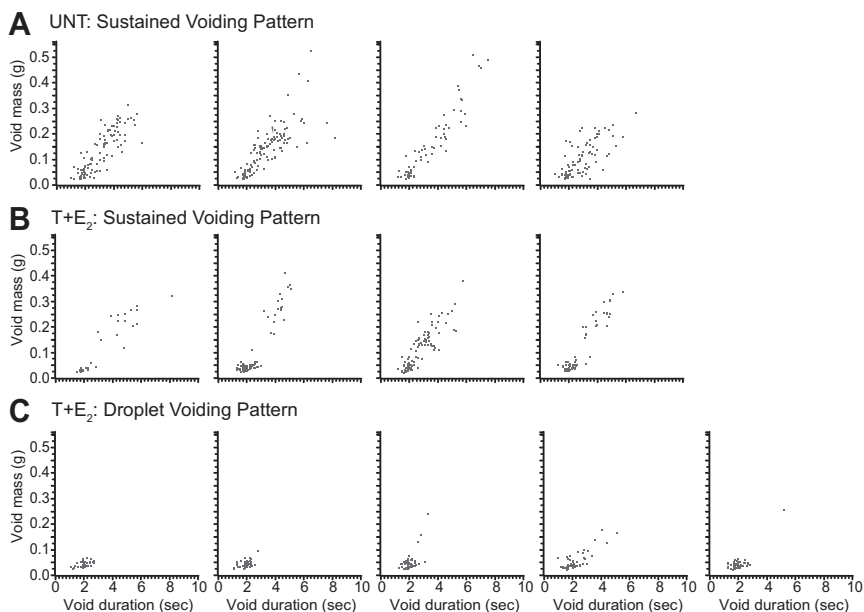
FIG. 4. Urinary voiding events across all sessions are plotted by void mass (grams) and void duration (seconds) for each BALB/c mouse (each *dot* represents a void). A, Individual voiding profiles show sustained voiding pattern in untreated (UNT) mice. B, Individual voiding profiles for four of nine mice treated with $T+E_2$ show a combination of sustained voiding and droplet voiding pattern, although some mice display sustained voids similar in duration and mass to untreated mice. C, Five of nine mice treated with $T+E_2$ demonstrate predominantly droplet voiding pattern.

Noninvasive study of urinary voiding behavior during hormone treatment revealed that some mice treated with $T+E_2$ developed droplet pattern voiding almost exclusively, likely a sign of end-stage BOO. Even among the mice treated with $T+E_2$ who did exhibit sustained voiding pattern, these mice also displayed droplet pattern voiding, suggesting that some degree of urinary voiding dysfunction was induced in all mice treated with $T+E_2$. These changes were reflected in the shorter void durations, smaller voided masses, and overall decrease in the number of sustained voids of mice treated with $T+E_2$ compared with untreated mice. Because our noninvasive uroflow method does not measure detrusor pressure, it is not possible to distinguish whether droplet voiding represents obstructive voiding (low flow in the setting of high detrusor pressure) or failure of coordinated detrusor contraction (low flow in the setting of low detrusor pressure). However, because of the noninvasive nature of our uroflow method, it does provide information relevant to understanding the voiding behavior associated with altered bladder function, which may be a better surrogate for LUTS. Moreover, it is not possible to establish in this model system a direct relationship among prostatic enlargement, BOO, and urinary voiding dysfunction. It is possible that changes in the compliance of the urethra could contribute to voiding dysfunction. Interestingly, in the hormone-treated mice with predominant droplet voiding pattern, mice were commonly observed hunching and apparently straining to void, which is a symptom reported by men with BPH. Mice treated with $T+E_2$ were also observed to have wet fur, suggesting that some droplets of urine were not measured in our noninvasive uroflow apparatus. Although overall the void durations were shorter among mice treated with $T+E_2$, the time to formation of the droplet in droplet voiding pattern may be underestimated.

In an individual patient, the development of obstructive complications such as urinary retention and upper urinary tract damage is difficult to predict. The natural history of BPH leading to BOO and LUTS in humans remains incompletely understood and is remarkably variable at the individual level (32). This variability is recapitulated in the $T+E_2$ mouse model. After 2 and 4 months of hormone treatment, all mice treated with T+E2 exhibited increased bladder mass and volume; however, after 4 months of hormone treatment, three of the nine mice treated with $T+E_2$ did not develop massively enlarged bladders. Furthermore, in uroflow experiments, four mice treated with $T+E_2$ exhibited some sustained voiding pattern that was not consistently different from untreated mice. However, even among the five of nine mice, there remained significantly fewer sustained voids, and overall, $T+E_2$ treatment caused decreased void duration and void mass. Although droplet voiding pattern is likely a sign of end-stage obstruction, we observed varying degrees of voiding dysfunction among all mice treated with $T+E_2$ when compared with untreated mice.

Animal models are powerful tools to address the etiology, natural history, and treatment of many disease processes. Treatment of male mice with $T+E_2$ induced a predictable sequence of changes in the bladder consistent with other models of mechanical BOO. In rabbit

TABLE 2. Effects of $T+E_2$ treatment on urinary void parameters in the male mouse

	UNT (n = 4)	T+E₂ (n = 9)
Voided mass (g)	2.99 ± 0.22	2.04 ± 0.14[a]
Void duration (sec)	0.13 ± 0.02	0.07 ± 0.01[a]
No. of sustained voids	53.5 ± 7.71	12.7 ± 5.17[a]

Values are means ± SEM. Sustained voids are defined as duration more than 3.0 sec and mass more than 0.10 g.

[a] $P < 0.01$ compared with untreated controls (UNT).

studies of partial BOO, the initial response of the bladder is a rapid increase in mass due to smooth muscle hypertrophy and gradual restoration of contractile function, followed by a compensatory stage in which the bladder mass stabilizes but the ability of the bladder to empty declines, with progressive, minor changes in the distribution of smooth muscle and collagen (33). In some rabbits with partial BOO, the bladder decompensates, heralded by a second increase in bladder mass as the muscle is replaced by connective tissue and paralleled by progressive deterioration of the bladder's ability to empty (10, 11, 33). Other models have suggested the hormonal underpinnings of BOO in male animals. Treatment of young dogs with androgens and estrogens suggest that these sex steroid hormones act synergistically to induce earlier and more extensive prostatic hyperplasia and resulting BOO (14). Monkeys treated with DHT and estradiol develop prostatic stromal hyperplasia (34). Among transgenic mice with the prolactin gene (*PRL*) overexpressed, the resulting hyperprolactinemia induces marked growth of the prostate in the setting of increased serum androgen levels (35). When *PRL* is overexpressed in a prostate-specific manner, the result is stromal hyperplasia and increased branching of prostatic ducts, without an increase in serum androgens (36). In contrast, among aromatase-overexpressing mice, only those with elevated serum E_2 and low serum T show urodynamic and anatomic evidence of BOO (37). However, unlike in mice treated with $T+E_2$, the aromatase-overexpressing mouse exhibits a decrease in thickness of the rhabdosphincter with urodynamic evidence of infravesical obstruction (37). In studies of the Noble rat, $T+E_2$ treatment that results in a decreased T to E_2 ratio causes prostatic inflammation and rhabdosphincter dysfunction, but importantly, these changes are not observed in rats treated with $T+E_2$ to induce a hyperandrogenic state (22, 23). Treatment of male Noble rats with $T+E_2$ for 6 wk causes modestly increased bladder mass, and $T+E_2$ treatment for 13 wk to induce hyperandrogenic state induces obstructive voiding in pressure-flow studies in parallel with inflammation in the dorsolateral prostate and periurethral prostate cancer (23, 38). The development of droplet voiding in mice treated with $T+E_2$ may represent obstruction, as suggested by urodynamic obstruction in the $T+E_2$-treated male Noble rat. In our model, decreased T to E_2 in a ratio designed to mimic physiological concentrations of older men induced benign enlargement of the prostate, urethral obstruction with static and possibly dynamic components, bladder complications, and voiding dysfunction suggestive of significant LUTS. Additionally, we observed new prostatic growth but not periurethral prostate cancer in mice. The $T+E_2$ mouse model is useful because it allows the assessment of how T and E_2 affect the prostate, bladder, and urethra in the context of a developmentally normal genitourinary tract. Furthermore, the hormonal induction of this model, which recreates a hormonal milieu similar to the aging man, is likely involved in the disease process found in men.

Male mice treated with $T+E_2$ develop a constellation of lower urinary tract abnormalities similar to those observed in men with BPH, including BOO, prostatic enlargement, ductal growth, and voiding dysfunction. Given that urinary tract complications are seen in models of mechanical BOO, and urethral narrowing was observed in $T+E_2$-treated mice, it is likely that bladder hypertrophy and enlargement is secondary to BOO. However, androgen and estrogen receptors are found not only in the prostate but also in other tissues of the male lower urinary tract, including the urethra and bladder (39). $T+E_2$ could act directly on extraprostatic cells and tissues in the lower urinary tract, causing bladder enlargement and voiding dysfunction independent of the prostatic growth effects. Given the wide range of tissues under the effects of systemic hormones, this is also possible in the complicated clinical scenario of patients with BPH and LUTS.

A hormonal etiology for BPH has long been proposed, but our understanding of the molecular basis continues to be limited. Induction of prostatic hyperplasia by treatment with androgens and estrogens has been well characterized in other model systems, but the power of mouse genetics makes the $T+E_2$ mouse model especially promising for elucidating the mechanism underlying hormonal induction of BPH, BOO, and voiding dysfunction. Future studies will use this model to evaluate genetic gain and loss of function with factors important in BPH and BOO as well as test pharmacological interventions important in the treatment or prevention of lower urinary tract abnormalities associated with hormonal changes in men as they age.

Acknowledgments

Address all correspondence and requests for reprints to: Department of Urology and Carbone Cancer Center, University of Wisconsin, 7107 Wisconsin Institute of Medical Re-

References

1. **Berry SJ, Coffey DS, Walsh PC, Ewing LL** 1984 The development of human benign prostatic hyperplasia with age. J Urol 132:474–479

2. **Roehrborn CG** 2005 Benign prostatic hyperplasia: an overview. Rev Urol 7 Suppl 9:S3–S14

3. **Oelke M, Kirschner-Hermanns R, Thiruchelvam N, Heesakkers J** 2012 Can we identify men who will have complications from benign prostatic obstruction (BPO)?: ICI-RS 2011. Neurourol Urodyn 31: 322–326

4. **Irwin DE, Milsom I, Kopp Z, Abrams P, Artibani W, Herschorn S** 2009 Prevalence, severity, and symptom bother of lower urinary tract symptoms among men in the EPIC study: impact of overactive bladder. Eur Urol 56:14–20

5. **Welch G, Weinger K, Barry MJ** 2002 Quality-of-life impact of lower urinary tract symptom severity: results from the Health Professionals Follow-up Study. Urology 59:245–250

6. **Parsons JK** 2010 Benign prostatic hyperplasia and male lower urinary tract symptoms: epidemiology and risk factors. Curr Bladder Dysfunct Rep 5:212–218

7. **Lee AJ, Garraway WM, Simpson RJ, Fisher W, King D** 1998 The natural history of untreated lower urinary tract symptoms in middle-aged and elderly men over a period of five years. Eur Urol 34:325–332

8. **Malkowicz SB, Wein AJ, Elbadawi A, Van Arsdalen K, Ruggieri MR, Levin RM** 1986 Acute biochemical and functional alterations in the partially obstructed rabbit urinary bladder. J Urol 136:1324–1329

9. **Bägli DJ, Joyner BD, Mahoney SR, McCulloch L** 1999 The hyaluronic acid receptor RHAMM is induced by stretch injury of rat bladder in vivo and influences smooth muscle cell contraction in vitro [corrected]. J Urol [Erratum (2003) 169:1090] 162:832–840

10. **Zderic SA, Wein A, Rohrman D, Gong C, Nigro D, Haugaard N, Levin R** 1998 Mechanisms of bladder smooth-muscle hypertrophy and decompensation: lessons from normal development and the response to outlet obstruction. World J Urol 16:350–358

11. **Austin JC, Chacko SK, DiSanto M, Canning DA, Zderic SA** 2004 A male murine model of partial bladder outlet obstruction reveals changes in detrusor morphology, contractility and Myosin isoform expression. J Urol 172:1524–1528

12. **Nicholson TM, Ricke WA** 2011 Androgens and estrogens in benign prostatic hyperplasia: past, present and future. Differentiation 82: 184–199

13. **Cunha GR, Hayward SW, Wang YZ, Ricke WA** 2003 Role of the stromal microenvironment in carcinogenesis of the prostate. Int J Cancer 107:1–10

14. **Coffey DS, Walsh PC** 1990 Clinical and experimental studies of benign prostatic hyperplasia. Urol Clin North Am 17:461–475

15. **Kaplan SA, Roehrborn CG, McConnell JD, Meehan AG, Surynawanshi S, Lee JY, Rotonda J, Kusek JW, Nyberg Jr LM** 2008 Long-term treatment with finasteride results in a clinically significant reduction in total prostate volume compared to placebo over the full range of baseline prostate sizes in men enrolled in the MTOPS trial. J Urol 180:1030–1032; discussion 1032–1033

16. **McConnell JD, Roehrborn CG, Bautista OM, Andriole Jr GL, Dixon CM, Kusek JW, Lepor H, McVary KT, Nyberg Jr LM, Clarke HS, Crawford ED, Diokno A, Foley JP, Foster HE, Jacobs SC, Kaplan SA, Kreder KJ, Lieber MM, Lucia MS, Miller GJ, Menon M, Milam DF, Ramsdell JW, Schenkman NS, Slawin KM, Smith JA** 2003 The long-term effect of doxazosin, finasteride, and combination therapy on the clinical progression of benign prostatic hyperplasia. N Engl J Med 349:2387–2398

17. **Morales A** 2002 Androgen replacement therapy and prostate safety. Eur Urol 41:113–120

18. **Harman SM, Metter EJ, Tobin JD, Pearson J, Blackman MR** 2001 Longitudinal effects of aging on serum total and free testosterone levels in healthy men. Baltimore Longitudinal Study of Aging. J Clin Endocrinol Metab 86:724–731

19. **Bélanger A, Candas B, Dupont A, Cusan L, Diamond P, Gomez JL, Labrie F** 1994 Changes in serum concentrations of conjugated and unconjugated steroids in 40- to 80-year-old men. J Clin Endocrinol Metab 79:1086–1090

20. **Bjørnerem A, Straume B, Midtby M, Fønnebø V, Sundsfjord J, Svartberg J, Acharya G, Oian P, Berntsen GK** 2004 Endogenous sex hormones in relation to age, sex, lifestyle factors, and chronic diseases in a general population: the Tromso Study. J Clin Endocrinol Metab 89:6039–6047

21. **Nilsson S, Gustafsson JÅ** 2011 Estrogen receptors: therapies targeted to receptor subtypes. Clin Pharmacol Ther 89:44–55

22. **Bernoulli J, Yatkin E, Talvitie EM, Santti R, Streng T** 2007 Urodynamic changes in a noble rat model for nonbacterial prostatic inflammation. Prostate 67:888–899

23. **Bernoulli J, Yatkin E, Konkol Y, Talvitie EM, Santti R, Streng T** 2008 Prostatic inflammation and obstructive voiding in the adult Noble rat: impact of the testosterone to estradiol ratio in serum. Prostate 68:1296–1306

24. **Ricke WA, McPherson SJ, Bianco JJ, Cunha GR, Wang Y, Risbridger GP** 2008 Prostatic hormonal carcinogenesis is mediated by in situ estrogen production and estrogen receptor alpha signaling. FASEB J 22:1512–1520

25. **Ricke WA, Ishii K, Ricke EA, Simko J, Wang Y, Hayward SW, Cunha GR** 2006 Steroid hormones stimulate human prostate cancer progression and metastasis. Int J Cancer 118:2123–2131

26. **Ricke WA, Wang Y, Kurita T, Hayward SW, Cunha GR** 2005 Hormonal and stromal regulation of normal and neoplastic prostatic growth. Prog Mol Subcell Biol 40:183–216

27. **Hedriana HL, Moore TR** 1994 Accuracy limits of ultrasonographic estimation of human fetal urinary flow rate. Am K Obstet Gynecol 171:989–992

28. **Wood RW, Baggs RB, Schwarz EM, Messing EM** 2006 Initial observations of reduced uroflow in transgenic adenocarcinoma of murine prostate. Urology 67:1324–1328

29. **Leung YY, Schwarz EM, Silvers CR, Messing EM, Wood RW** 2004 Uroflow in murine urethritis. Urology 64:378–382

30. **Valenstein ES, Cox VC, Kakolewski JW** 1967 Polydipsia elicited by

the synergistic action of a saccharin and glucose solution. Science 157:552–554

31. **Landau EH, Jayanthi VR, Churchill BM, Shapiro E, Gilmour RF, Khoury AE, Macarak EJ, McLorie GA, Steckler RE, Kogan BA** 1994 Loss of elasticity in dysfunctional bladders: urodynamic and histochemical correlation. J Urol 152:702–705

32. **Lepor H** 2004 Pathophysiology, epidemiology, and natural history of benign prostatic hyperplasia. Rev Urol 6(Suppl 9):S3–S10

33. **Levin RM, Hudson AP** 2004 The molecular genetic basis of mitochondrial malfunction in bladder tissue following outlet obstruction. J Urol 172:438–447

34. **Jeyaraj DA, Udayakumar TS, Rajalakshmi M, Pal PC, Sharma RS** 2000 Effects of long-term administration of androgens and estrogen on rhesus monkey prostate: possible induction of benign prostatic hyperplasia. J Androl 21:833–841

35. **Wennbo H, Kindblom J, Isaksson OG, Törnell J** 1997 Transgenic mice overexpressing the prolactin gene develop dramatic enlargement of the prostate gland. Endocrinology 138:4410–4415

36. **Kindblom J, Dillner K, Sahlin L, Robertson F, Ormandy C, Törnell J, Wennbo H** 2003 Prostate hyperplasia in a transgenic mouse with prostate-specific expression of prolactin. Endocrinology 144:2269–2278

37. **Streng T, Li X, Lehtoranta M, Mäkelä S, Poutanen M, Talo A, Tekmal RR, Santti R** 2002 Infravesical obstruction in aromatase over expressing transgenic male mice with increased ratio of serum estrogen-to-androgen concentration. J Urol 168:298–302

38. **Bosland MC, Ford H, Horton L** 1995 Induction at high incidence of ductal prostate adenocarcinomas in NBL/Cr and Sprague-Dawley Hsd:SD rats treated with a combination of testosterone and estradiol-17β or diethylstilbestrol. Carcinogenesis 16:1311–1317

39. **Chavalmane AK, Comeglio P, Morelli A, Filippi S, Fibbi B, Vignozzi L, Sarchielli E, Marchetta M, Failli P, Sandner P, Saad F, Gacci M, Vannelli GB, Maggi M** 2010 Sex steroid receptors in male human bladder: expression and biological function. J Sex Med 7:2698–2713

THE ENDOCRINE SOCIETY®

Save the Date for ENDO 2013
June 15 - 18, 2013, San Francisco, California
www.endo-society.org/endo2013